

# The formation of close binary systems by dynamical interactions and orbital decay

Matthew R. Bate,<sup>1,2\*</sup> Ian A. Bonnell,<sup>3</sup> and Volker Bromm.<sup>2,4</sup>

<sup>1</sup>*School of Physics, University of Exeter, Stocker Road, Exeter EX4 4QL*

<sup>2</sup>*Institute of Astronomy, University of Cambridge, Madingley Road, Cambridge CB3 0HA*

<sup>3</sup>*School of Physics and Astronomy, University of St Andrews, North Haugh, St Andrews, Fife, KY16 9SS*

<sup>4</sup>*Harvard-Smithsonian Center for Astrophysics, 60 Garden Street, Cambridge, MA 02138, U.S.A.*

Accepted for publication in MNRAS

## ABSTRACT

We present results from the first hydrodynamical star formation calculation to demonstrate that close binary stellar systems (separations  $\lesssim 10$  AU) need not be formed directly by fragmentation. Instead, a high frequency of close binaries can be produced through a combination of dynamical interactions in unstable multiple systems and the orbital decay of initially wider binaries. Orbital decay may occur due to gas accretion and/or the interaction of a binary with its circumbinary disc. These three mechanisms avoid the problems associated with the fragmentation of optically-thick gas to form close systems directly. They also result in a preference for close binaries to have roughly equal-mass components because dynamical exchange interactions and the accretion of gas with high specific angular momentum drive mass ratios towards unity. Furthermore, due to the importance of dynamical interactions, we find that stars with greater masses ought to have a higher frequency of close companions, and that many close binaries ought to have wide companions. These properties are in good agreement with the results of observational surveys.

**Key words:** accretion, accretion discs – binaries: close – binaries: spectroscopic – circumstellar matter – hydrodynamics – stars: formation

## 1 INTRODUCTION

The process of star formation preferentially produces binary stellar systems (e.g. Duquennoy & Mayor 1991). The favoured mechanism for explaining this high frequency of binaries is the collapse and fragmentation of molecular cloud cores (e.g. Boss & Bodenheimer 1979; Boss 1986; Bonnell et al. 1991; Nelson & Papaloizou 1993; Burkert & Bodenheimer 1993; Bate, Bonnell & Price 1995). However, while fragmentation can readily create wide binary systems (separations  $\gtrsim 10$  AU), there are severe difficulties with fragmentation producing close binaries directly. This is a significant deficiency since approximately 20% of solar-type stars have main-sequence companions that orbit closer than 10 AU (Duquennoy & Mayor 1991), and the frequency of massive spectroscopic binaries appears to be even higher (Garmany, Conti & Massey 1980; Abt et al. 1990; Morrell & Levato 1991; Mason et al. 1998).

As a molecular cloud core begins to collapse, the formation of wide binaries through fragmentation is possible because the gas easily radiates away the gravitational poten-

tial energy that is released. The gas remains approximately isothermal and, thus, the Jeans mass decreases with density as  $\rho^{-1/2}$ . However, at densities of  $\gtrsim 10^{-13}$  g cm<sup>-3</sup> or  $n(\text{H}_2) \gtrsim 10^{10}$  cm<sup>-3</sup> (Larson 1969; Masunaga & Inutsuka 2000) the rate of heating from dynamical collapse exceeds the rate at which the gas can cool. The gas heats up, and the Jeans mass begins to increase so that a Jeans-unstable region of gas becomes Jeans-stable. This results in the formation of a pressure-supported fragment with a mass of several Jupiter-masses and a radius of  $\approx 5$  AU (Larson 1969). Fragmentation on smaller scales is inhibited by thermal pressure. Therefore, initial binary separations must be  $\gtrsim 10$  AU. The formation of such pressure-supported fragments is frequently referred to as the opacity limit for fragmentation (Low & Lynden-Bell 1976; Rees 1976) and may set a lower limit to the mass of brown dwarfs (Boss 1988; Bate, Bonnell & Bromm 2002).

A possibility for fragmentation at higher densities (hence on smaller length scales) exists when the pressure-supported fragment has accreted enough material for its central temperature to exceed 2000 K. At this temperature, molecular hydrogen begins to dissociate, which provides a way for the release of gravitational energy to be absorbed

\* E-mail: mbate@astro.ex.ac.uk

without significantly increasing the temperature of the gas. Thus, a nearly isothermal second collapse occurs within the fragment that ultimately results in the formation of a stellar core with radius  $\approx 1R_{\odot}$  (Larson 1969). Several studies have investigated the possibility that fragmentation during this second collapse forms close binary systems directly (Boss 1989; Bonnell & Bate 1994; Bate 1998, 2002). Boss (1989) found that fragmentation was possible during this second collapse, but that the fragments spiralled together due to gravitational torques and did not survive. Bonnell & Bate (1994) found that fragmentation to form close binaries and multiple systems could occur in a disc that forms around the stellar core. However, both these studies began with somewhat arbitrary initial conditions for the pressure-supported fragment. Bate (1998) performed the first three-dimensional calculations to follow the collapse of a molecular cloud core through the formation of the pressure-supported fragment, the second collapse, and the formation of the stellar core and its surrounding disc. In these and subsequent calculations (Bate 2002), Bate found that the second collapse did not result in sub-fragmentation due to the high thermal pressure and angular momentum transport via gravitational torques.

In this paper, we present results from the first hydrodynamical star formation calculation to produce dozens of stars and brown dwarfs while simultaneously resolving beyond the opacity limit for fragmentation. Despite the fact that no close binaries (separations  $\lesssim 10$  AU) are formed by direct fragmentation, we find that the calculation eventually produces several close binary systems through a combination of dynamical interactions in multiple systems, and the orbital decay of wide binaries via gas accretion and their interactions with circumbinary discs.

The paper is structured as follows. In section 2, we briefly describe the numerical method and the initial conditions for our calculation. In section 3, we present results from our calculation and compare them with observations. Finally, in section 4, we give our conclusions.

## 2 COMPUTATIONAL METHOD AND INITIAL CONDITIONS

The calculation presented here was performed using a three-dimensional, smoothed particle hydrodynamics (SPH) code. The SPH code is based on a version originally developed by Benz (Benz 1990; Benz et al. 1990). The smoothing lengths of particles are variable in time and space, subject to the constraint that the number of neighbours for each particle must remain approximately constant at  $N_{\text{neigh}} = 50$ . We use the standard form of artificial viscosity (Monaghan & Gingold 1983) with strength parameters  $\alpha_v = 1$  and  $\beta_v = 2$ . Further details can be found in Bate et al. (1995). The code has been parallelised by M. Bate using OpenMP.

### 2.1 Opacity limit for fragmentation and the equation of state

To model the opacity limit for fragmentation without performing full radiative transfer, we use a barotropic equation of state for the thermal pressure of the gas  $p = K\rho^\eta$ , where  $K$  is a measure of the entropy of the gas. The value of the effective polytropic exponent  $\eta$ , varies with density as

$$\eta = \begin{cases} 1, & \rho \leq 10^{-13} \text{ g cm}^{-3}, \\ 7/5, & \rho > 10^{-13} \text{ g cm}^{-3}. \end{cases} \quad (1)$$

We take the mean molecular weight of the gas to be  $\mu = 2.46$ . The value of  $K$  is defined such that when the gas is isothermal  $K = c_s^2$ , with the sound speed  $c_s = 1.84 \times 10^4 \text{ cm s}^{-1}$  at 10 K, and the pressure is continuous when the value of  $\eta$  changes.

This equation of state reproduces the temperature-density relation of molecular gas during spherically-symmetric collapse (as calculated with frequency-dependent radiative transfer) to an accuracy of better than 20% in the non-isothermal regime up to densities of  $10^{-8} \text{ g cm}^{-3}$  (Masunaga & Inutsuka 2000). Thus, our equation of state should model collapsing regions well, but may not model the equation of state in protostellar discs particularly accurately due to their departure from spherical symmetry.

### 2.2 Sink particles

The opacity limit results in the formation of distinct pressure-supported fragments in the calculation. As these fragments accrete, their central density increases, and it becomes computationally impractical to follow their internal evolution until they undergo the second collapse to form stellar cores because of the short dynamical time-scales involved. Therefore, when the central density of a pressure-supported fragment exceeds  $\rho_s = 10^{-11} \text{ g cm}^{-3}$ , we insert a sink particle into the calculation (Bate et al. 1995). The gas within radius  $r_{\text{acc}} = 5$  AU of the centre of the fragment (i.e. the location of the SPH particle with the highest density) is replaced by a point mass with the same mass and momentum. Any gas that later falls within this radius is accreted by the point mass if it is bound and its specific angular momentum is less than that required to form a circular orbit at radius  $r_{\text{acc}}$  from the sink particle. Thus, gaseous discs around sink particles can only be resolved if they have radii  $\gtrsim 10$  AU. Sink particles interact with the gas only via gravity and accretion.

Since all sink particles are created from pressure-supported fragments, their initial masses are  $\approx 10$  Jupiter-masses ( $M_J$ ), as given by the opacity limit for fragmentation (Boss 1988). Subsequently, they may accrete large amounts of material to become higher-mass brown dwarfs ( $\lesssim 75 M_J$ ) or stars ( $\gtrsim 75 M_J$ ), but all the stars and brown dwarfs begin as these low-mass pressure-supported fragments.

The gravitational acceleration between two sink particles is Newtonian for  $r \geq 4$  AU, but is softened within this radius using spline softening (Benz 1990). The maximum acceleration occurs at a distance of  $\approx 1$  AU; therefore, this is the minimum separation that a binary can have even if, in reality, the binary's orbit would have been hardened.

Replacing the pressure-supported fragments with sink particles is necessary in order to perform the calculation. However, it is not without a degree of risk. If it were possible to follow the fragments all the way to stellar densities (as done by Bate 1998) and still follow the evolution of the large-scale cloud over its dynamical time-scale, we might find that a few of the objects that we replace with sink particles merge together or are disrupted by dynamical interactions. We have tried to minimise the degree to which this may occur by insisting that the central density of

the pressure-supported fragments exceeds  $\rho_s$  before a sink particle is created. This is two orders of magnitude higher than the density at which the gas is heated and ensures that the fragment is self-gravitating, centrally-condensed and, in practice, roughly spherical before it is replaced by a sink particle. In theory, it would be possible for a long collapsing filament to exceed this density over a large distance, thus making the creation of one or more sink particles ambiguous. However, the structure of the collapsing gas that results from the turbulence prohibits this from occurring; no long roughly uniform-density filaments with densities  $\approx \rho_s$  form during the calculation. Furthermore, each pressure-supported fragment must undergo a period of accretion before its central density exceeds  $\rho_s$  and it is replaced by a sink particle. For example, it is common in the calculation to be able to follow a pressure-supported fragment that forms via gravitational instability in a disc for roughly half an orbital period before it is replaced. Thus, the fragments do have some time in which they may be disrupted or merge. Only occasionally during the calculation are low-mass pressure-supported fragments disrupted; most are eventually replaced by sink particles.

### 2.3 Initial conditions

The initial conditions consist of a large-scale, turbulent molecular cloud. The cloud is spherical and uniform in density with a mass of  $50 M_\odot$  and a diameter of  $0.375$  pc ( $77400$  AU). At the temperature of  $10$  K, the mean thermal Jeans mass is  $1 M_\odot$  (i.e. the cloud contains  $50$  thermal Jeans masses). The free-fall time of the cloud is  $t_{\text{ff}} = 6.0 \times 10^{12}$  s or  $1.90 \times 10^5$  years.

Although the cloud is uniform in density, we impose an initial supersonic turbulent velocity field on it in the same manner as Ostriker, Stone & Gammie (2001). We generate a divergence-free random Gaussian velocity field with a power spectrum  $P(k) \propto k^{-4}$ , where  $k$  is the wavenumber. In three dimensions, this results in a velocity dispersion that varies with distance,  $\lambda$ , as  $\sigma(\lambda) \propto \lambda^{1/2}$  in agreement with the observed Larson scaling relations for molecular clouds (Larson 1981). The velocity field is normalised so that the kinetic energy of the turbulence equals the magnitude of the gravitational potential energy of the cloud. The initial root-mean-square Mach number of the turbulence is  $\mathcal{M} = 6.4$ .

### 2.4 Resolution

The local Jeans mass must be resolved throughout the calculation to model fragmentation correctly (Bate & Burkert 1997; Truelove et al. 1997; Whitworth 1998; Boss et al. 2000). Bate & Burkert (1997) found that this requires  $\gtrsim 2N_{\text{neigh}}$  SPH particles per Jeans mass;  $N_{\text{neigh}}$  is insufficient. We have repeated their calculation using different numbers of particles and find that  $1.5N_{\text{neigh}} = 75$  particles is also sufficient to resolve fragmentation (Bate, Bonnell & Bromm, in preparation). The minimum Jeans mass in the calculation presented here occurs at the maximum density during the isothermal phase of the collapse,  $\rho = 10^{-13}$  g cm $^{-3}$ , and is  $\approx 0.0011 M_\odot$  ( $1.1 M_J$ ). Thus, we use  $3.5 \times 10^6$  particles to model the  $50 M_\odot$  cloud. In fact, a gas clump with the above mass and density could not collapse because

as soon as it was compressed it would heat up (equation 1) and would no longer contain a Jeans mass. Therefore, in practice, any collapsing gas clump in the simulation contains many more SPH particles than the ‘minimum’ Jeans mass above. This SPH calculation is one of the largest ever performed. It required approximately  $95000$  CPU hours on the SGI Origin 3800 of the United Kingdom Astrophysical Fluids Facility (UKAFF).

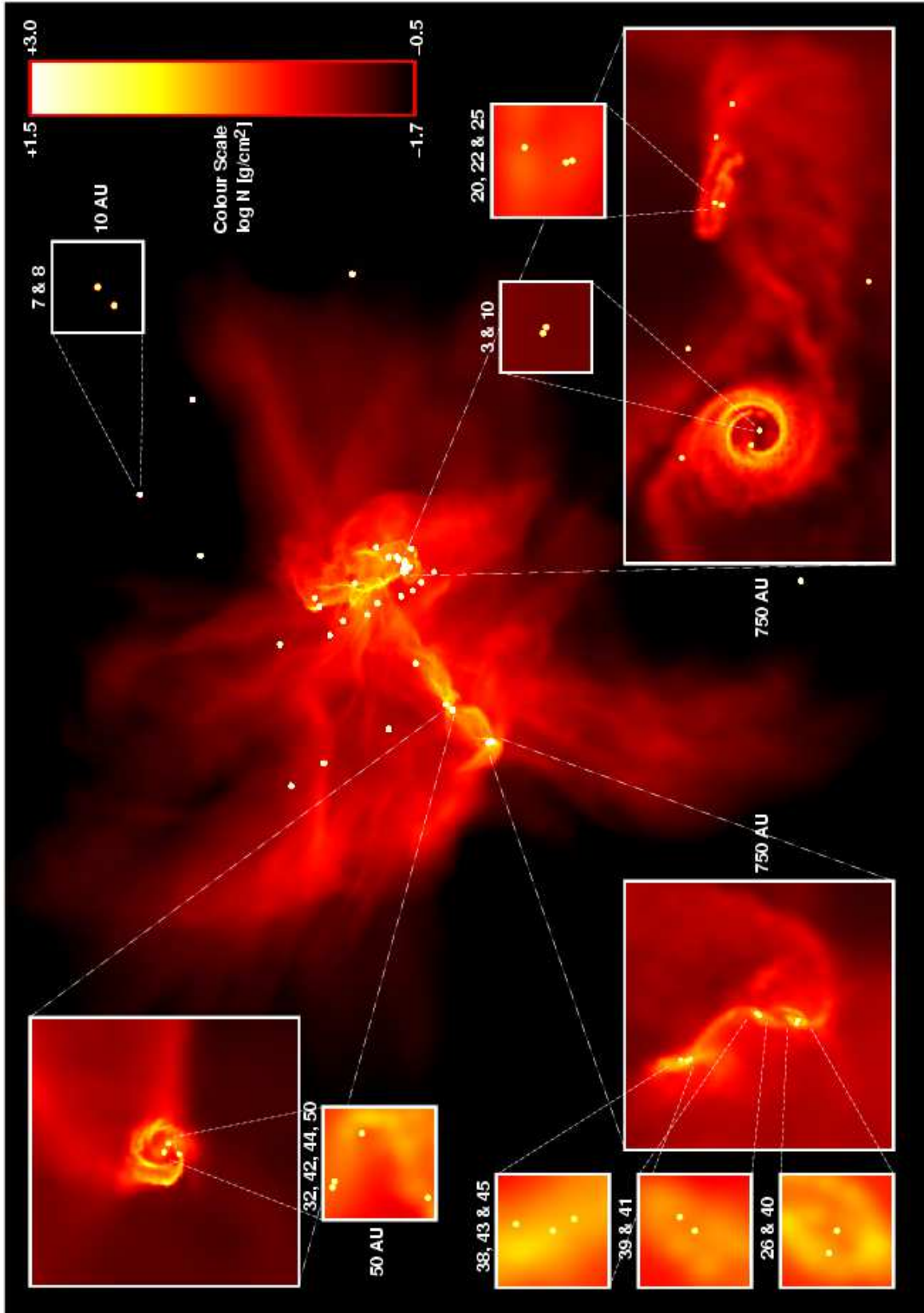
## 3 RESULTS

### 3.1 Evolution of the cloud

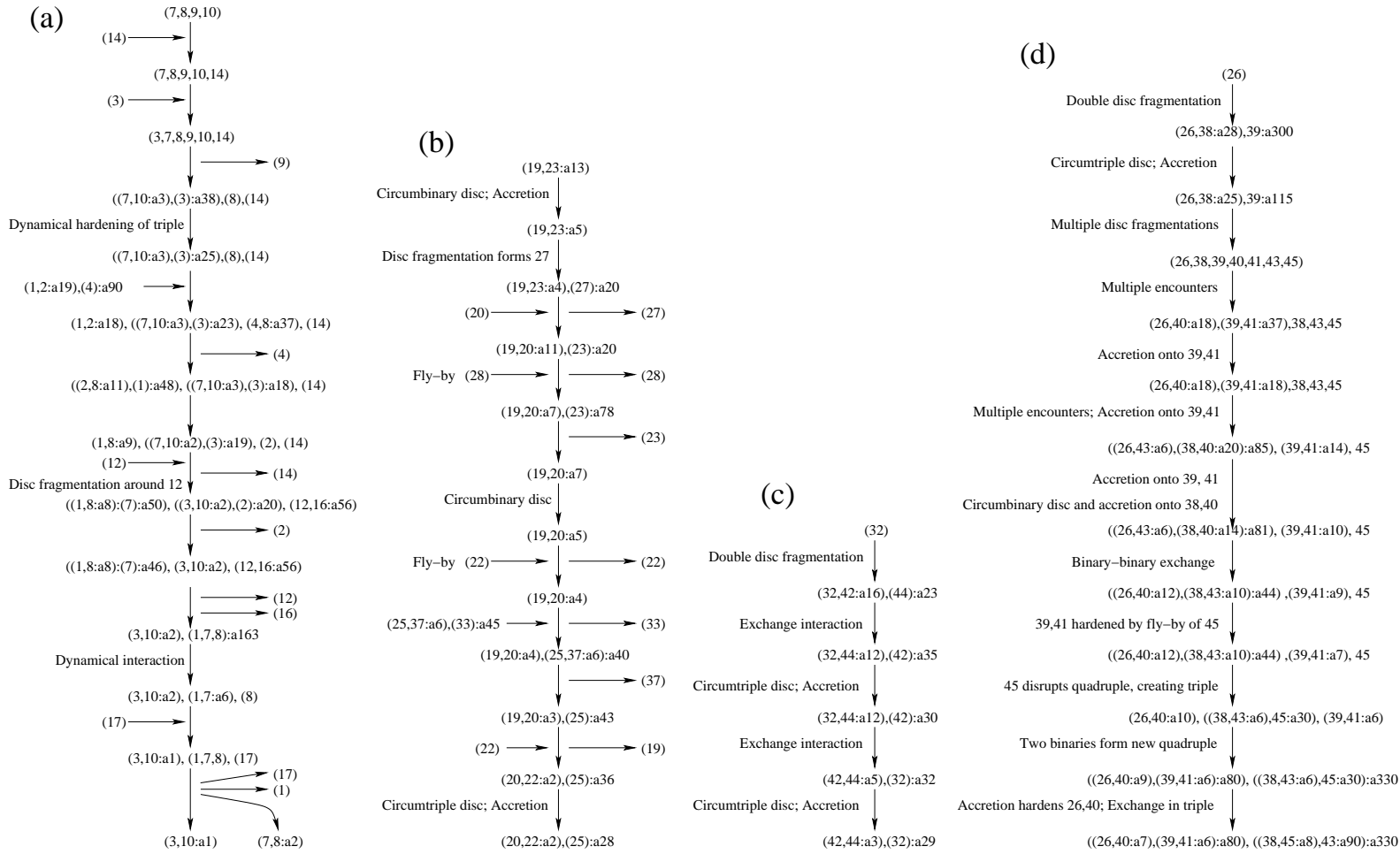
The hydrodynamical evolution of the cloud produces shocks which decrease the turbulent kinetic energy initially supporting the cloud. In parts of the cloud, gravity begins to dominate and dense self-gravitating cores form and collapse. These dense cores are the sites where the formation of stars and brown dwarfs occurs. Although the cloud initially contains more than enough turbulent energy to support itself against gravity, this turbulence decays on the dynamical time-scale of the cloud and star formation begins after just one global free-fall time at  $t = 1.04t_{\text{ff}}$  (i.e.  $t = 1.97 \times 10^5$  yrs). This rapid decay of the turbulence is consistent with other numerical studies of turbulence in molecular clouds (e.g. MacLow et al. 1998; Stone, Ostriker & Gammie 1998; Ostriker et al. 2001). We followed the calculation for  $\approx 69000$  years after the star formation began until  $t = 1.40t_{\text{ff}}$  ( $t = 2.66 \times 10^5$  yrs). At this point we had exhausted our allocation of computer time and the calculation was stopped.

Figure 1 illustrates the state of the cloud at the end of the calculation. The star formation occurs in three main dense cores within the cloud, resulting in three stellar groups. These groups are composed of single, binary and higher-order systems that were produced via a combination of the fragmentation of collapsing gas filaments (whose collapse is halted when the gas heats up at high densities; Inutsuka & Miyama 1992), the fragmentation of massive circumstellar discs (e.g. Bonnell 1994; Whitworth et al. 1995; Burkert, Bate, & Bodenheimer 1997), and star-disc capture (Larson 1990; Clarke & Pringle 1991a,b). At any particular time, the largest of the stellar groups contains no more than  $\approx 20$  objects. Thus, the groups dissolve quickly. In fact, the time-scales for star formation within the dense cores and the dissolution of the groups are both  $\approx 2 \times 10^4$  years. Thus, the stellar groups undergo chaotic evolution with stars and brown dwarfs being ejected from the cloud even as new objects are forming. If the calculation were followed until well after star formation had ceased, all of the groups would dissolve on time-scales of a few tens of thousands of years.

When the calculation is stopped, the cloud has produced  $23$  stars and  $18$  brown dwarfs. An additional  $9$  objects have substellar masses, but are still accreting. Three of these would probably end up with substellar masses if the calculation were continued, but the other six are likely to become stars. The formation mechanism of the brown dwarfs in this calculation has been discussed by Bate et al. (2002). The evolution of the cloud and the properties of the stars and brown dwarfs will be discussed in detail in subsequent papers. In this paper, we concentrate on the mechanism by which the close binary systems form.



**Figure 1.** The locations and states of the 7 close binary systems when the simulation was stopped ( $t = 1.40t_{\text{ff}} = 2.66 \times 10^5$  yr). Most of the close binaries remain members of multiple systems and are surrounded by discs, although one (top right) has been ejected from the cloud and does not have a resolved disc. Star formation occurs in three dense cores. The colour scales show the logarithm of column density with  $-1.7 < \log N < 1.5$  for the main picture and  $-0.5 < \log N < 3.0$  for each of the inserts. The main picture is  $\approx 80000$  AU from top to bottom. The dimensions of the inserts are given in AU (inserts of equal size have equal dimensions). The numbers identifying the objects pictured in the 10-AU and 50-AU inserts are given above each insert to allow comparison with Table 1 and Figure 2.



**Figure 2.** Diagrams showing the sequences of events leading to the formation of the 7 close binary systems in the course of the calculation. Time increases in each sequence from top to bottom. Causes of evolution (such as another object falling into a system, or the interaction of the system with a circumbinary disc) and ejected objects (if any) are given to the left and right of each sequence, respectively. Groups of objects and hierarchical multiple systems are indicated by the use of parentheses. For example, (7,8,9,10,14) indicates 5 objects in a group with no obvious hierarchy. Another example is ((7,10:a3),(3):a38),(8),(14) which indicates a binary composed of objects 7 and 10 with a semi-major axis of 3 AU with a companion (object 3) in an orbit with a 38-AU semi-major axis. In turn, this hierarchical triple system ((7,10:a3),(3):a38) is part of a larger-scale group consisting of the triple system and objects 8 and 14.

Binary	$M_1$ $M_\odot$	$M_2$ $M_\odot$	$q$	$a$ AU	Notes and the end of the calculation
3,10	0.73	0.41	0.56	1.1*	In hierarchical triple, 0.083 $M_\odot$ at 28 AU; circumtriple disc; member of a bound group
7,8	0.53	0.24	0.44	2.0*	Ejected from cloud
20,22	0.35	0.11	0.33	2.2*	In hierarchical triple, 0.23 $M_\odot$ at 28 AU; circumtriple disc; member of a bound group
26,40	0.13	0.039	0.29	6.7	Circumbinary disc; member of septuple system with (39,41), ((45,38),43)
39,41	0.070	0.047	0.67	5.7	Circumbinary disc; member of septuple system with (26,40), ((45,38),43)
42,44	0.10	0.095	0.93	2.6*	In unstable quintuple system; circumquadruple disc
45,38	0.083	0.079	0.96	8.8	In hierarchical triple, 0.022 $M_\odot$ at 90 AU; circumtriple disc; member of septuple system

**Table 1.** The properties of the 7 close binary systems at the end of the calculation. The numbers identifying the individual stars or brown dwarfs from which the binary systems are composed are allocated in order of their formation. We list the masses of the two components  $M_1$  and  $M_2$ , the mass ratio  $q$ , and the semi-major axis  $a$ . Note that the mass ratios tend to be high, with no values less than  $q = 0.29$  and most greater than  $q = 1/2$ . Asterisks indicate when the semi-major axis is less than the gravitational softening length. If gravitational softening had not been used, these systems may have been hardened further.

### 3.2 The formation of close binary systems

When the calculation is stopped, amongst the 50 stars and brown dwarfs, there are 7 close binary systems with separations less than 10 AU (Table 1 and Figures 1 and 2). Six of these close binaries are members of unstable multiple systems, but one has been ejected from the cloud on its own and will evolve no further (Figures 1 and 2).

As described in the introduction, it seems that binaries with separations  $\lesssim 10$  AU cannot form by direct fragmentation because fragmentation is halted by the formation of pressure-supported fragments with radii of  $\approx 5$  AU. Our calculation models this opacity limit for fragmentation and, as expected, none of the fragments in our calculation form closer than  $\approx 10$  AU from each other. The three smallest separations between any existing object and a forming fragment are 9, 21, and 22 AU and only the last of these ends up in a close binary system. What mechanism(s) produce the 7 close binary systems in our calculation?

In Figure 2, we trace the histories of the stars and brown dwarfs that play a role in producing each of the 7 close binary systems. We find that the close binary systems are produced as a natural consequence of the evolution of wide binaries and multiple systems in a gas-rich environment. Three processes are involved: the accretion of gas, the interaction of a binary or triple with its circumbinary or circumtriple disc, and dynamical interactions between objects.

#### 3.2.1 Accretion

Accretion aids in the production of close binaries in two main ways. First, accretion onto a binary can decrease its separation (e.g. Figure 3; Figure 2d, steps 5–7). This effect of gas accretion on the orbital separation of a binary has been studied extensively (Artymowicz 1983; Bate 1997; Bate & Bonnell 1997; Bate 2000). Bate & Bonnell (1997) show that accretion onto a binary from a gaseous envelope decreases the orbital separation of a binary unless the specific angular momentum of the accreted gas is significantly greater than that of the binary. If a binary accretes a large amount of material compared to its initial mass (e.g. a factor  $\gtrsim 10$ ) this can easily reduce the separation of the binary by 1–2 orders of magnitude (Bate 2000).

Second, accretion can similarly destabilise stable hierarchical multiple systems by reducing the separation of wide

components (e.g. Figure 4; Figure 2b, step 11; Figure 2c, steps 3 and 5; Figure 2d, step 2). This and other effects of accretion on the stability and mass ratios of triple systems were studied by Smith, Bonnell & Bate (1997). The destabilisation of multiple systems contributes to the production of close binaries because it forces the system to undergo dynamical interactions (section 3.2.3).

#### 3.2.2 Circumbinary and circumtriple discs

If a binary is surrounded by a circumbinary disc, gravitational torques from the binary transfer angular momentum from the binary’s orbit into the disc, causing the binary’s components to spiral together (Artymowicz et al. 1991; Bate & Bonnell 1997). Thus, a wide binary can be hardened into a close binary (e.g. Figure 5; Figure 2b, steps 1 and 6; Figure 2d, step 7). Similarly, a disc around a hierarchical triple can reduce the separation of the wide companion, destabilising the system (e.g. Figures 4 and 6; Figure 2b, step 11; Figure 2c, steps 3 and 5; Figure 2d, step 2).

Such disc interactions are very efficient; even relatively low-mass discs can have a significant effect over time (Pringle 1991). The circumbinary and circumtriple discs in this calculation frequently contain a significant fraction of the system’s mass as can be observed by the spiral density waves caused by gravitational instabilities within them (Figures 1, 3, 5, and 6). This makes it difficult to separate the effects of accretion and gravitational torques, but, in any case, these discs play an important role in reducing the separations of binaries and triples.

#### 3.2.3 Dynamical interactions

Dynamical interactions can lead to the orbital evolution of a binary in several ways. If the orbital velocity of a binary is greater than the velocity of an incoming object while it is still at a great distance (i.e. the binary is ‘hard’), the binary will survive the encounter (Hut & Bahcall 1983). However, several outcomes are possible. The binary may simply be hardened by the encounter, with the single object removing energy and angular momentum. Alternately, if the encounter is sufficiently close, an unstable multiple system will be formed. Its chaotic evolution will usually lead to the ejection of the object with the lowest mass. If the ejected object

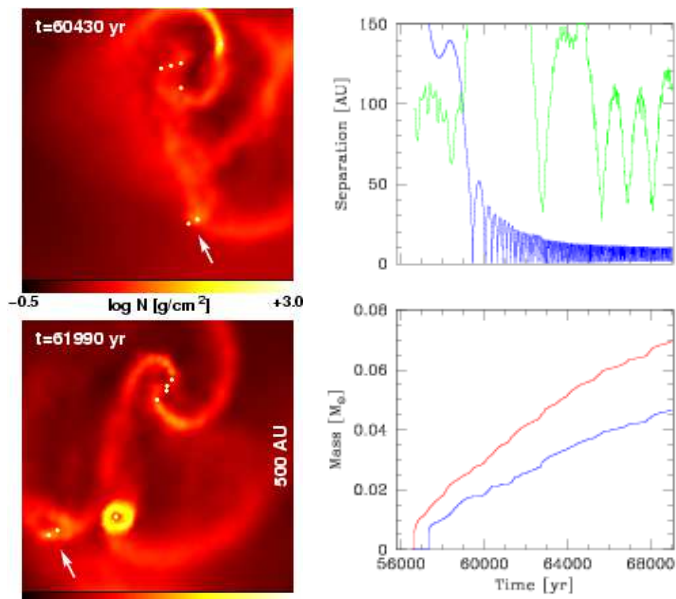


**Figure 3.** As an example of the way in which accretion can harden the orbit of a binary, we present the evolution of brown dwarfs 39 and 41 versus time (see also Figure 2d, steps 5–7). Left panels: column density  $\log N$  at two times during the evolution. The binary, consisting of objects 39 & 41, is indicated by the arrow. Top-right panel: the separation of brown dwarfs 39 & 41 (blue) and the distance between brown dwarf 39 and the closest object apart from 41 (green). Bottom-right panel: the masses of 39 (red) and 41 (blue). Dynamical interactions in an unstable multiple system force 39 and 41 to form an eccentric binary system with a semi-major axis of  $\approx 37$  AU at  $t \approx 59000$  yrs. Over the next 5000 years, accretion reduces the semi-major axis of this binary by nearly an order of magnitude. Dynamical interactions have only a minimal effect on the binary’s separation during this period (as shown by the green line). Note that object 39 has a mass of  $0.070 M_{\odot}$  at the end of the calculation (Table 1) and would probably enter the stellar-mass regime if the calculation were continued. The final mass of object 41 is unclear. Time is given in years after the onset of star formation (star formation begins at  $t = 1.04t_{\text{ff}} = 1.97 \times 10^5$  yrs).

was a component of the original binary, the net effect is an exchange interaction.

The suggestion that dynamical encounters play an important role in the formation of close binaries has been made by Tokovinin (1997, 2000), who observed that many close binaries have wider companions (see below). In the calculation discussed here, dynamical encounters play the dominant role in producing close binaries (e.g. Figure 6 and the exchange interactions, hardening by fly-bys, and binary-binary interactions described in Figure 2). However, it is important to note that N-body dynamical interactions alone cannot produce the high frequency of close binaries that we obtain. Indeed, Kroupa & Burkert (2001) find that N-body calculations which begin with star clusters (100 to 1000 stars) consisting entirely of binaries with periods  $4.5 < \log(P/\text{days}) < 5.5$  produce almost no binaries with periods  $\log(P/\text{days}) < 4$ . Similarly, the dissolution of small-N clusters typically results in binaries with separations only an order of magnitude smaller than the size of the initial cluster (Sterzik & Durisen 1998).

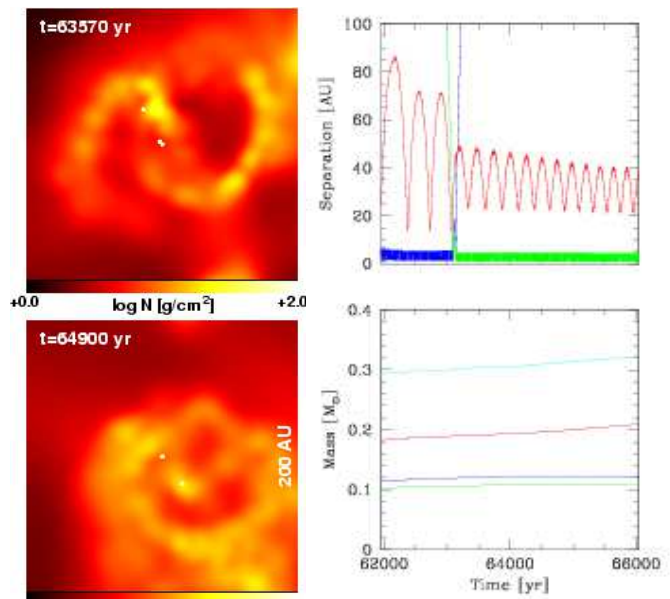


**Figure 4.** An example of the way in which gravitational torques and accretion from a circumtriple disc can alter the orbit of a triple system. Left panels: column density  $\log N$  at two times during the evolution. Top-right panel: the separations of stars 19 (blue), 22 (green), and 25 (red) from star 20. Bottom-right panel: the masses of stars 19 (blue), 20 (cyan), 22 (green), and 25 (red). A triple system consisting of a close binary (stars 19 and 20) and a wide companion (star 25) undergoes an exchange interaction at  $t \approx 63000$  yr in which star 19 is ejected and replaced by star 22. Subsequently, the system evolves only through its interaction with the circumtriple disc which decreases the semi-major axis of star 25’s orbit around the close binary (stars 20 and 22) from 36 to 28 AU (see also Figure 2b, steps 10 and 11). Note that the circumtriple disc contains a significant fraction of the system’s mass and is subject to gravitational instabilities, as demonstrated by the spiral density waves. Time is given in years after the onset of star formation.

The key difference in this calculation is the effect of the gas-rich environment. Along with the effects from accretion and circumbinary/circumtriple discs discussed above, the presence of gas allows dynamical encounters to be dissipative and to transport angular momentum. Such dissipative encounters include star-disc encounters (Larson 1990; Clarke & Pringle 1991a,b; McDonald & Clarke 1995; Hall, Clarke & Pringle 1996), where the dissipation of kinetic energy allows the formation of bound systems from objects that would otherwise be unbound, and other tidal interactions (Larson 2002).

### 3.3 The resulting properties of close binary systems

As mentioned above, dynamical exchange interactions typically lead to the ejection of the least massive component. Thus, if a binary encounters a star whose mass is in between the masses of the binary’s components, the binary’s secondary will usually be replaced and the binary’s mass ratio will be equalised. In addition, gas with high specific angular momentum that accretes from a circumbinary disc or a gaseous envelope onto a binary, is preferentially cap-



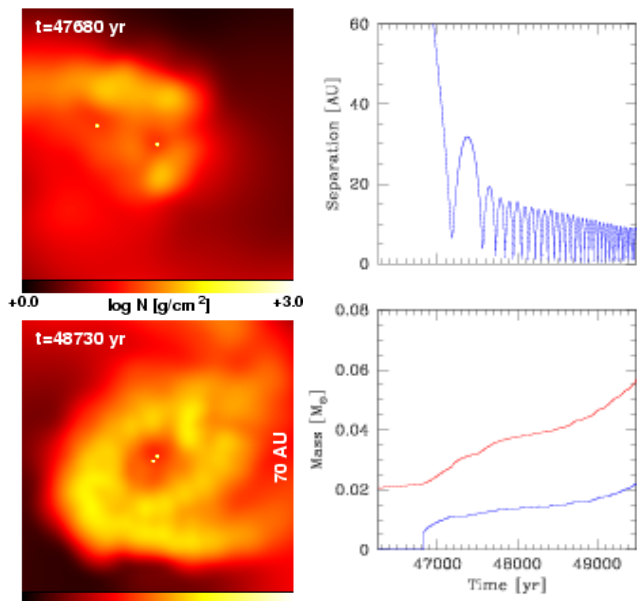


**Figure 5.** An example of the way in which gravitational torques and accretion from a circumbinary disc can harden the orbit of a binary (see also Figure 2b, step 1). Left panels: column density  $\log N$  at two times during the evolution. Right-panels: the evolution of the separation and masses of brown dwarfs 19 (red) and 23 (blue) versus time. Time is given in years after the onset of star formation.

tured by the secondary and, thus, also drives the mass ratio towards unity (Artymowicz 1983; Bonnell & Bastien 1992; Whitworth et al. 1995; Bate & Bonnell 1997; Bate 2000). Even if accretion comes from a relatively slowly rotating cloud, the long-term effect of this accretion is usually to equalise the binary’s components (Bate 2000). Thus, each of the mechanisms involved in producing close binaries favours the production of equal-mass systems. This is reflected in the mass ratios of the seven close binary systems that form in our calculation (Table 1), all of which have values  $q \gtrsim 0.3$  and most of which have  $q > 1/2$ . Thus, the observational result that close binaries (periods  $\lesssim 10$  years) tend to have higher mass ratios than wider binaries (Mazeh et al. 1992; Halbwachs, Mayor & Udry 1998; Tokovinin 2000) is explained naturally if these processes are an integral part of the formation mechanism for close binaries.

Overall, the calculation produces 7 close binaries among 50 stars and brown dwarfs, giving a close-binary fraction of  $7/43 = 16\%$ . Given the small numbers, this is in good agreement with the observation that  $\approx 20\%$  of solar-type stars have a less massive main-sequence companion within 10 AU (Duquennoy & Mayor 1991). Thus, dynamical encounters and orbital decay can produce the observed frequency of close binaries.

However, because dynamical exchange interactions preferentially select the two most massive objects, another consequence of the way in which close binaries form is that the frequency of close binaries increases with the mass of the primary. This can be understood by considering a binary and an incoming object whose mass is greater than either of the two components of the binary. In this case, the typical result is that the incoming object and the primary from the orig-

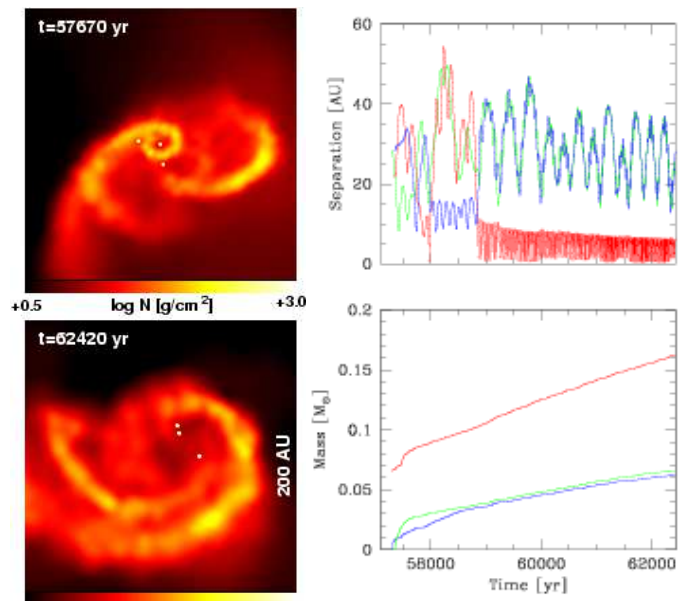


**Figure 6.** An example of how a combination of dynamical interactions, the interaction of a triple system with a disc, and accretion can produce close binaries (see also Figure 2c). Left panels: column density  $\log N$  at two times during the evolution. Bottom-right panel: the masses of objects 32 (red), 42 (green), and 44 (blue) versus time. Top-right panel: the separations of stars 32 & 42 (blue), 32 & 44 (green), and 42 & 44 (red). An unstable triple system consisting of a 16-AU binary (stars 32 & 42) and a wide companion (star 44) undergoes an exchange interaction at  $t \approx 58000$  yr to produce a hierarchical triple consisting of a 12-AU binary (stars 32 & 44) and star 42 in a 35-AU orbit. The wide companion’s orbit decays due to its interaction with a circumbinary disc, forcing a second exchange interaction that leaves stars 42 and 44 in a 5-AU binary and star 32 in a 32-AU orbit. Subsequent interaction with the circumbinary disc hardens the triple and accretion hardens the close binary. Note that continued accretion eventually results in three stellar-mass objects (Table 1). Time is given in years after the onset of star formation.

inal binary form a new binary. After several such exchange interactions, the mass of the primary in the new binary can be much greater than the original primary’s mass. In the calculation presented here, the dependence of the frequency of close binaries on stellar mass is quite strong. Of  $\approx 20$  brown dwarfs, there is only one binary brown dwarf system (and if the calculation were followed further, at least one of the components would probably accrete into the stellar regime), while of the 11 stars with masses  $> 0.2 M_{\odot}$ , 5 are members of close binary systems. While it is difficult to extrapolate from our low-mass star-forming cloud to larger star clusters and more massive stars, this trend of an increasing frequency of close binaries with stellar mass is supported by observational surveys (Garmany et al. 1980; Abt et al. 1990; Morrell & Levato 1991; Mason et al. 1998).

Finally, we note that at the end of the calculation, only one of our close binaries has been ejected from the cloud and is on its own. The others remain members of larger-scale bound groups and three are members of hierarchical triple systems (Table 1; Figure 1). This large number of wider companions is yet another indication of the importance of multiple systems in producing close binaries. Even



allowing for the eventual dissolution of the bound groups, it seems likely that some of the hierarchical triple systems will survive. Although the true frequency of wide companions to close binaries is not yet well known, many close binaries do have wider components (e.g. Mayor & Mazeh 1987; Tokovinin 1997, 2000). Indeed, it was this observation that led Tokovinin (1997) to propose that dynamical interactions in multiple systems may play an important role in the formation of close binary systems. Further surveys to determine the true frequency of wide companions to close binary systems would be invaluable.

#### 4 CONCLUSIONS

We have presented results from a hydrodynamic calculation of the collapse and fragmentation of a turbulent molecular cloud to form 50 stars and brown dwarfs. The calculation mimics the opacity limit for fragmentation by using a barotropic equation of state to model the heating of collapsing gas at high densities. This results in a minimum mass of  $\approx 10$  Jupiter masses for the lowest-mass brown dwarfs (see Bate et al. 2002) and prevents fragmentation on scales smaller than  $\approx 10$  AU. Despite this lower limit on the initial minimum separation between fragments, we find that as the stellar groups and unstable multiple systems evolve in the gas-rich environment, a high frequency of close binary systems (separations  $\lesssim 10$  AU) is produced.

Examining the history of these close binary systems, we find that they are formed through a combination of dynamical interactions in unstable multiple systems, and orbital decay due to accretion and/or the interaction of binary and triple systems with circumbinary and circumtriple discs. These formation mechanisms allow realistic numbers of close binary systems to be produced without the need for fragmentation on length scales  $< 10$  AU. This avoids the difficulties associated with the fragmentation of optically-thick gas during the collapse initiated by the dissociation of molecular hydrogen (Boss 1989; Bonnell & Bate 1994; Bate 1998, 2002).

As a consequence of the dependence of close binary formation on dynamical exchange interactions and the accretion of material with high specific angular momentum, we find that close binaries tend not to have extreme mass ratios. All of our systems have mass ratios  $q \gtrsim 0.3$ . Furthermore, the frequency of close binaries is dependent on mass in that massive stars are more likely to have close companions than lower mass stars. These properties are in good agreement with the results of observational surveys. At the end of our calculation, many of the close binaries are members of hierarchical triple systems. Although these systems may not yet have finished evolving, the implication is that many close binaries ought to have wider companions. Recent observations support this hypothesis, but larger surveys to determine the frequency of wide companions to close binary systems are necessary to demonstrate it conclusively.

#### ACKNOWLEDGMENTS

The computations reported here were performed using the UK Astrophysical Fluids Facility (UKAFF). VB ac-

knowledges support by the European Community's Research Training Network under contract HPRN-CT-2000-0155, Young Stellar Clusters.

#### REFERENCES

- Abt H. A., Gomez A. E., Levy S. G., 1990, *ApJS*, 74, 551  
 Artymowicz P., 1983, *Acta Astronomica*, 33, 223  
 Artymowicz P., Clarke C. J., Lubow S. H., Pringle J. E., 1991, *ApJ*, 370, L35  
 Bate M. R., 1997, *MNRAS*, 285, 16  
 Bate M. R., 1998, *ApJ*, 508, L95  
 Bate M. R., 2000, *MNRAS*, 314, 33  
 Bate M. R., 2002, in preparation  
 Bate M. R., Bonnell I. A., 1997, *MNRAS*, 285, 33  
 Bate M. R., Bonnell I. A., Bromm V., 2002, *MNRAS*, in press  
 Bate M. R., Bonnell I. A., Price N. M., 1995, *MNRAS*, 277, 362  
 Bate M. R., Burkert A., 1997, *MNRAS*, 288, 1060  
 Benz W., 1990, in Buchler J. R., ed., *The Numerical Modeling of Nonlinear Stellar Pulsations: Problems and Prospects*. Kluwer, Dordrecht, p. 269  
 Benz W., Bowers R. L., Cameron A. G. W., Press W., 1990, *ApJ*, 348, 647  
 Bonnell I., Bastien P., 1992, *ApJ*, 401, 654  
 Bonnell I. A., 1994, *MNRAS*, 269, 837  
 Bonnell I. A., Bate M. R., 1994, *MNRAS*, 271, 999  
 Bonnell I., Martel H., Bastien P., Arcoragi J.-P., Benz W., 1991, *ApJ*, 377, 553  
 Boss A. P., 1986, *ApJS*, 62, 519  
 Boss A. P., 1988, *ApJ*, 331, 370  
 Boss A. P., 1989, *ApJ*, 346, 336  
 Boss A. P., Bodenheimer P., 1979, *ApJ*, 234, 289  
 Boss A. P., Fisher R. T., Klein R. I., McKee C. F., 2000, *ApJ*, 528, 325  
 Burkert A., Bodenheimer P., 1993, *MNRAS*, 264, 798  
 Burkert A., Bate, M. R., Bodenheimer P., 1997, *MNRAS*, 289, 497  
 Clarke C. J., Pringle J. E., 1991a, *MNRAS*, 249, 584  
 Clarke C. J., Pringle J. E., 1991b, *MNRAS*, 249, 588  
 Duquennoy A., Mayor M., 1991, *A&A*, 248, 485  
 Garmany C. D., Conti P. S., Massey P., 1980, *ApJ*, 242, 1063  
 Halbwachs J. L., Mayor M., Udry S., 1998, in Rebolo R., Martin E. L., Zapatero Osorio M.R., eds., *Brown Dwarfs and Extrasolar Planets (ASP Conf. Ser. 134)*. Brigham Young University, Provo, p. 308  
 Hall S. M., Clarke C. J., Pringle J. E., 1996, *MNRAS*, 278, 303  
 Hut P., Bahcall J. N., 1983, *ApJ*, 268, 319  
 Inutsuka S., Miyama S. M., 1992, *ApJ*, 388, 392  
 Kroupa P., Burkert A., 2001, *ApJ*, 555, 945  
 Larson R. B., 1969, *MNRAS*, 145, 271  
 Larson R. B., 1981, *MNRAS*, 194, 809  
 Larson R. B., 1990, in Cappuzzo-Dolcetta R., Chiosi C., di Fazio A., eds, *Physical Processes in Fragmentation and Star Formation*. Kluwer, Dordrecht, P. 389  
 Larson R. B., 2002, *MNRAS*, 332, 155  
 Low C., Lynden-Bell D., 1976, *MNRAS*, 176, 367  
 McDonald J. M., Clarke C. J., 1995, *MNRAS*, 275, 671  
 MacLow M. M., Klessen R. S., Burkert A., Smith M. D., Kessel O., 1998, *Phys. Rev. Lett.*, 80, 2754  
 Mason B. D., Gies D. R., Hartkopf W. I., Bagnuolo W. G. Jr., Brummelaar T. T., McAlister H. A., 1998, *AJ*, 115, 821  
 Masunaga H., Inutsuka S., 2000, *ApJ*, 531, 350  
 Mayor M., Mazeh T., 1987, *A&A*, 171, 157  
 Mazeh T., Goldberg D., Duquennoy A., Mayor M., 1992, *ApJ*, 401, 265  
 Monaghan J. J., Gingold R. A., 1983, *J. Comput. Phys.*, 52, 374  
 Morrell N., Levato H., 1991, *ApJS*, 75, 965

- Nelson R., Papaloizou J. C., 1993, MNRAS, 265, 905  
Ostriker E. C., Stone J. M., Gammie C. F., 2001, ApJ, 546, 980  
Pringle J. E., 1991, MNRAS, 248, 754  
Rees M. J., 1976, MNRAS, 176, 483  
Smith K. W., Bonnell I. A., Bate M. R., 1997, MNRAS, 288, 1041  
Sterzik M. F., Durisen R. H., 1998, A&A, 339, 95  
Stone J. M., Ostriker E. C., Gammie C. F., 1998, ApJ, 508, L99  
Tokovinin A. A., 1997, AstL, 23, 727  
Tokovinin A. A., 2000, A&A, 360, 997  
Truelove J. K., Klein R. I., McKee C. F., Holliman J. H.II, Howell  
L. H., Greenough J. A., Woods D. T., 1998, ApJ, 495, 821  
Whitworth A. P., 1998, MNRAS, 296, 442  
Whitworth A. P., Chapman S. J., Bhattal A. S., Disney M. J.,  
Pongracic H., Turner J. A., 1995, MNRAS, 277, 727